THE JOURNAL OF PHYSICAL CHEMISTRY B

Article

pubs.acs.org/JPCB

In Situ Study of Dynamic Conformational Transitions of a Water-Soluble Poly(3-hexylthiophene) Derivative by Surfactant Complexation

Cameron D. Danesh, Nathan S. Starkweather, and Shanju Zhang*

Department of Chemistry and Biochemistry, California Polytechnic State University, San Luis Obispo, California 93407, United States

ABSTRACT: Transitions in the backbone conformation of polythiophenes (PTs) in organic solvents, measurable spectroscopically, have been widely observed to influence thin-film morphology; however, such conformational transitions of water-soluble PT derivatives, with respect to their *intra*molecular versus *inter*molecular origin, remain largely obscure. Here, we report on dynamic conformational transitions of poly(3-potassium hexanoate thiophene) in aqueous cetyltrimethylammonium bromide investigated by means of Fourier transform infrared spectroscopy, differential scanning calorimetry, polarizing optical microscopy, and ultraviolet−visible absorption and fluorescence spectroscopy. As-prepared complexes exist as stable hydrogels. Upon dilution, a significant time-dependent chromism occurs spontaneously. A coil-to-rod conformational transition is identified in this mechanism. Study into the corresponding kinetics demonstrates an inverse first-order rate law. It is found that the conformational transition is thermally reversible and concentration-independent. The critical transition temperature is largely dependent on the surfactant architecture. A theoretical model is presented to explain this new phenomenon and the mechanisms behind its influence on the optoelectronic properties.

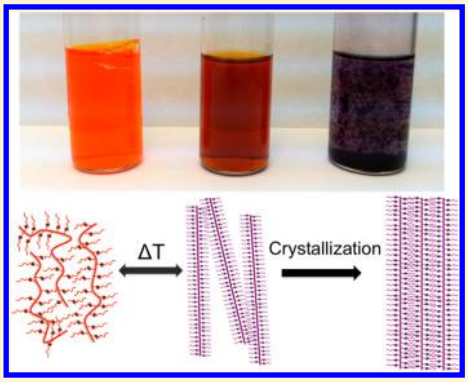

INTRODUCTION

Conjugated polymers have shown promise in the development of flexible electronic devices via low-cost, solution-based processing techniques because of their unique combination of polymer mechanical flexibility and excellent photophysical properties.[1−3] The incorporation of flexible side chains with the conjugated backbone has been widely employed to improve polymer processability in organic media.[4−6] A well-studied system is poly(3-alkylthiophene)s (P3ATs), which possess high charge carrier mobility and low bandgap. For instance, poly(3-hexylthiophene) (P3HT) has become a benchmark material employed in the active layer of polymer photovoltaic devices.[7−11] In a good organic solvent, P3HT exhibits a coil-like conformation. Upon addition of a poor solvent, the polymer chains spontaneously change from coil-like conformations to rod-like aggregates, followed by the formation of crystalline nanowires.[12−15] It has been recognized that the P3HT nanowires play a crucial role in the production of high-efficiency photovoltaic devices.[16−19]

The solvents employed contribute greatly to the emission of volatile organic compounds when scaling up manufacturing processes, an issue of great concern in modern industrial settings. Charged conjugated polymers, so-called conjugated polyelectrolytes (CPEs), however, are in general water-soluble because of their ionic moieties in side chains.[20−26] For this reason, CPEs have been paid great attention recently for widespread applications ranging from chemical and biological sensors to organic solar cells. Controlling the behavior of these polymers in aqueous solution over a broad range of concentrations is fundamental to process design in the development of functional materials. To this end, ionic surfactants, as additives to counterionic CPEs, have been employed in the preparation of novel water-soluble supramolecular complexes via electrostatic interactions. Recently, highly ordered columnar mesophases have been reported in aqueous P3AT complexes.[27] The use of ordered mesophases could generate improved morphology in the films processed from their lyotropic solution for enhanced device performance.[28] It has been recognized that surfactant complexation results in an alteration of CPE's optoelectronic properties. This phenomenon is termed "surfactochromism".[29−32]

In general, CPEs are present as loose aggregates in aqueous solution, with ionic side chains facing the water−polymer interface and $\pi-\pi$ stacking between the backbones within.[33] Surfactants induce the disruption of these aggregates, accompanied by the enhancement of fluorescence emission and the quantum yield.[29,31−34] Many factors, such as the backbone structure of CPEs,[19,35,36] the surfactant lipophile length,[33] the molar ratio between surfactants and CPEs,[24,31,32] and overall surfactant concentration,[33,37] play a role in altering the optoelectronic properties. Because of complicated interplay among various intra- and interchain interactions, the physical

Received: August 4, 2012
Revised: September 29, 2012
Published: October 5, 2012

origin of surfactochromism is still far from being understood and is yet to be described unambiguously.

In this work, we report for the first time on the kinetics and thermodynamics of surfactochromism of poly[3-(potassium-6-hexanoate)thiophene-2,5-diyl] (P3KHT) in aqueous cetyltrimethylammonium bromide (CTAB) in the dilute regime. P3KHT is a recently developed carboxylated P3HT and possesses a bandgap similar to that of its parent material, demonstrating great potential for green processing in the production of various electronic devices.[38−41] A coil-to-rod transition of single polymer chains is identified upon diluting as-prepared hydrogels. We put forward arguments to explain the dilution-induced conformational transitions of the complex.

EXPERIMENTAL METHODS

Regioregular (82−90% head-to-tail) poly[3-(potassium-6-hexanoate)thiophene-2,5-diyl] (P3KHT, average M_w = 60 kg/mol, Rieke Metals Inc.), cetyltrimethylammonium bromide (CTAB, Sigma Alrdich), and dihexadecyl dimethyl ammonium bromide (DHAB, Sigma Aldrich) were used as received, in preparation of the supramolecular complexes. Stock solutions with nominal concentrations of 0.05 M (corresponding to the 1:1 molar ratio of the cationic surfactant and anionic polymer repeat unit) were prepared in nanopure water (Milli-Q, 18 MΩ) by dropwise addition of homogeneous surfactant solutions to polyelectrolyte solutions. Three hours of microcentrifugation (18-Centrifuge Biotechnical Services Inc.) at 14 000 rpm produced a hydrogel of the complexes, as shown in Scheme 1c.

Scheme 1. (a) Illustration of Complexation between a Conjugated Polyelectrolyte and a Surfactant, (b) Chemical Structures of the P3KHT and CTAB, and (c) Photographs of the Concentrated Aqueous Pure P3KHT and P3KHT-CTAB Complex after Centrifugation

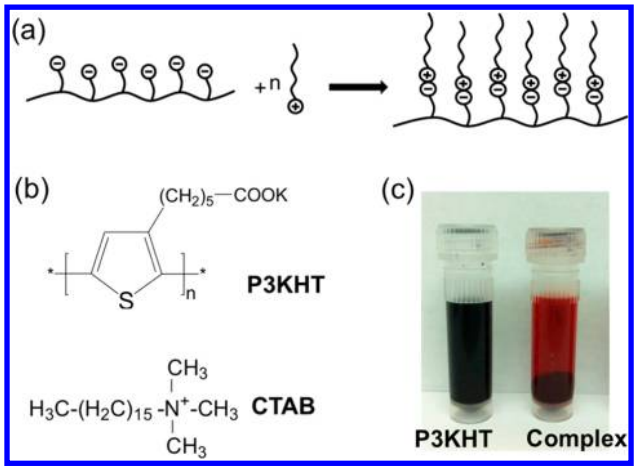

Spectroscopic measurements of aqueous solutions were performed by serial dilution of the isolated stock supernatants; concentrations noted in this study are in terms of the monomeric repeat unit (the carboxylate molarity). UV−vis absorbance and fluoresence spectra were obtained under stirring cuvettes on a Jasco V-550 spectrophotometer and Jasco FP-6500 spectrofluorometer, respectively. Both instruments employed temperature-control fixtures, and samples were closed from the ambient atmosphere during measurement. Stock solutions were directly oven-heated at 60 °C for 48 h to produce solids for differential scanning calorimetry (DSC) measurements at 5 °C/min under nitrogen flow, using TA Instruments DSC Q200. Drop-cast films of 0.5 mM solutions were prepared at room-temperature for 48 h for measurements performed on a Nicolet 380 Fourier transform infrared (FT-IR) spectrometer and for visualization by polarizing optical microscopy with a Leica DM2500 P.

RESULTS AND DISCUSSION

Complexation. The preparation of the complexes yielded stable hydrogels, which are distinctly different from either the polyelectrolyte P3KHT or surfactant CTAB solutions. Macroscopic phase separation of the hydrogel was observed upon centrifugation (Scheme 1). The phase separation is attributed to the inherent polydispersity of the commercial polymer. Similar separation behavior has been recently reported for polythiophene−surfactant complex hydrogels[27] and has been widely observed for liquid crystalline polymers.[42] The isolated supernatant is the focus of this study; however, no differences in the spectroscopic and thermal properties were observed between the two phases.

Figure 1a shows the UV−vis absorption spectra of the P3KHT aqueous solution in the presence of various amounts of CTAB. The control P3KHT in water displays an absorption maximum at 560 nm with a strong vibronic absorption at 590 nm. This fine structure has been widely observed in aggregated polythiophenes and corresponds to the Franck−Condon progression of the C=C stretching mode within the thiophene ring.[13,31,43] Addition of the CTAB produces a pronounced blue shift of the absorption maximum demonstrating the formation of P3KHT-CTAB complexes.[27] The blue shift of the absorption maximum is attributed to the breakup of P3KHT aggregates due to the incorporation of the long alkyl side chains.[27] The disappearance of the vibronic fine structure further indicates the disruption of ring stacking.[31,43] This argument is supported by the fluorescence data, as shown in Figure 1b. The fluorescence of the control P3KHT in water was completely quenched over a wide concentration range from micromolar to millimolar, with no detectable emission intensity at all excitation wavelengths from 400 to 700 nm. Such photoquenching is indicative of intermolecular interactions that allow for charge transfer and result in nonradiative electronic processes.[44,45] Addition of CTAB to the aqueous P3KHT yields a suppression of photoquenching. With an increasing amount of CTAB, the emission intensity is enhanced and the fluoresence bands progressively narrow. These findings are consistent with the breakup of aggregates in solution.[29] Moreover, addition of the CTAB results in a slight shift of the emission maximum toward lower wavelength. The surfactant-induced hypsochromic shift of absorbance and the enhancement of fluorescence in this system are in good agreement with other conjugated polymer complexes in literature.[27]

Confirmation of the quaternary ammonium−carboxylate ionic bonding is further confirmed in the dried film of the stoichiometric complex using FTIR and DSC, as shown in Figure 2. FT-IR data show alterations in the vibrational energies of methylene bending bands (2800−3000 cm^{-1}) as well as the carboxylate stretching bands (1300−1600 cm^{-1}). The slight blue shifts in methylene vibrations and the substantial reduction in peak half-width are attributed to the improved packing of the aliphatic side chains in the complex films.[46] DSC heating curves show that the control P3KHT exhibits only a glass transition at T_g = 70 °C while the P3KHT-CTAB complex shows a sharp

dx.doi.org/10.1021/jp307728r | J. Phys. Chem. B 2012, 116, 12887−12894

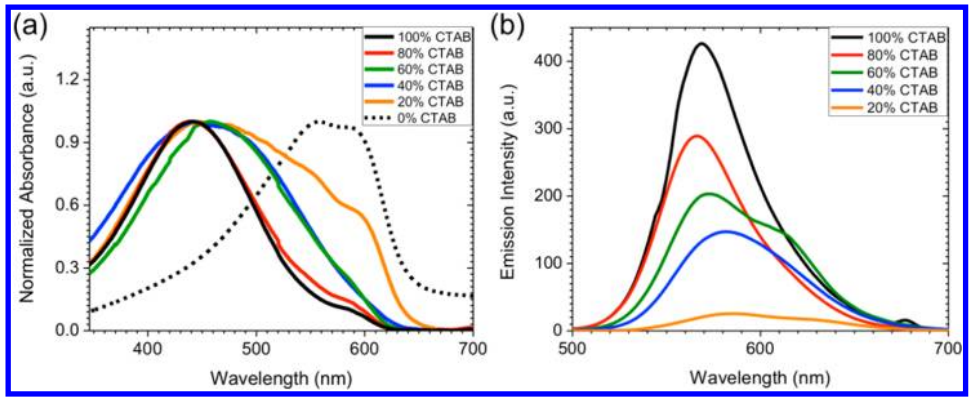

Figure 1. (a) Normalized UV−vis absorption and (b) fluoresence spectra of aqueous P3KHT complexes with various amounts of CTAB. The concentration is 4×10^{-5} M. The excitation wavelength of fluorescence is 430 nm.

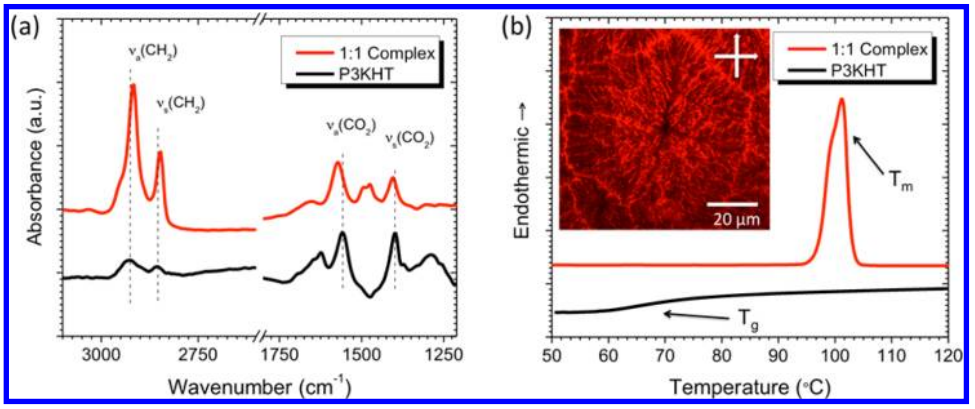

Figure 2. (a) FTIR spectra and (b) DSC curves of pristine P3KHT and the P3KHT-CTAB stoichiometric complex. The inset is an optical image of spherulites of the complex under crossed polarizers.

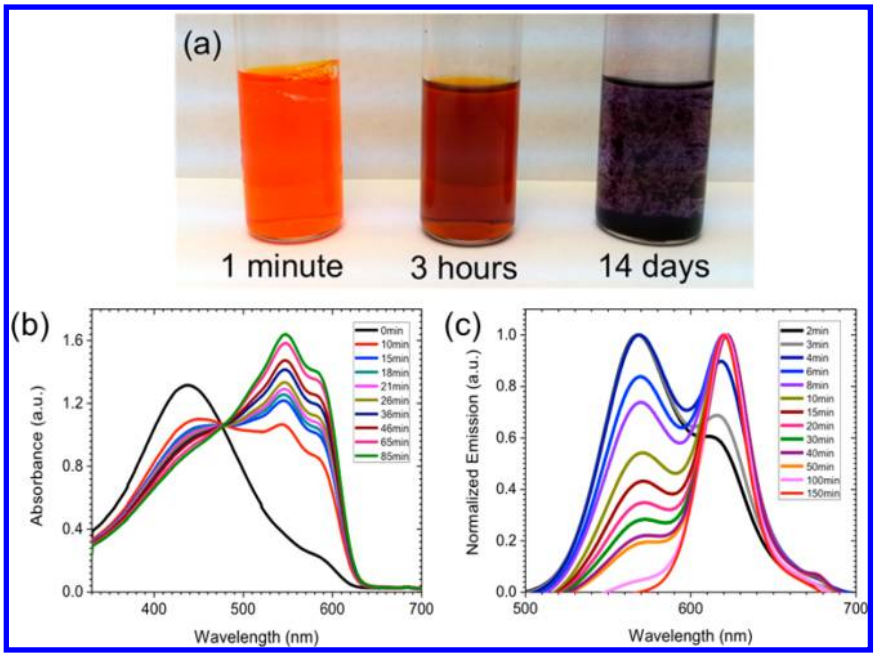

Figure 3. Time-dependent chromism of newly diluted P3KHT−CTAB complex solution at 25 °C. (a) The color changes with aging time, and eventual precipitation, of the aqueous complex over a period of weeks after dilution (5.4×10^{-4} M). (b) UV−vis absorption and (c) normalized fluoresence spectra (λ_{exc} = 560 nm). The concentration is 4×10^{-5} M.

melting transition at T_m = 102 °C. The crystalline behavior of the P3KHT-CTAB complex is further evidenced by the optical texture of spherulites, characteristic of semicrystalline polymers[47] (inset of Figure 2b).

dx.doi.org/10.1021/jp307728r | J. Phys. Chem. B 2012, 116, 12887−12894

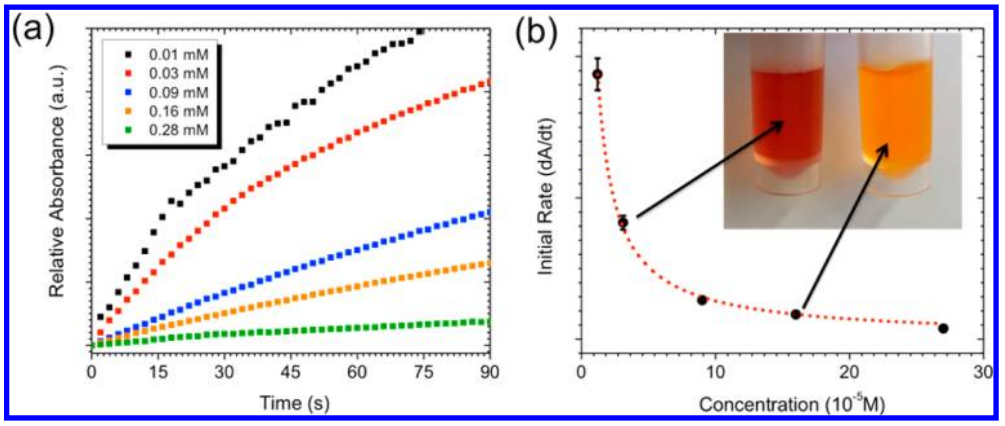

Figure 4. Kinetics of the coil-to-rod transition of the aqueous P3KHT−CTAB complexes. (a) Time-dependent absorbance at λ = 590 nm with respect to concentration at 25 °C. (b) The data of initial rate against concentration. The dotted line is a power-law fit with an exponent of 0.98 ± 0.01. The uncertainty in the initial rate for each concentration results from its regression error taken over the first 90 s. Images (inset) are taken 90 s after dilution corresponding to the indicated solution concentration.

Conformational Transition. The as-prepared complex was a stable hydrogel (Scheme 1c). Surprisingly, the system gradually altered color from orange to brown upon dilution, and eventual precipitates were observed after weeks, as shown in Figure 3a. Figure 3b and c show the time-dependent spectroscopic properties of the diluted solution of the stoichiometric complex. The absorbance of the freshly diluted complex appears with a λ_{max} of 430 nm (Figure 3b); however, a subsequent 120 nm shift toward higher wavelengths occurs spontaneously over an aging period at room temperature. A distinct isosbestic point is observed, indicating that two phases exist in the solution.[12,48] They are identified as twisted coil-like and planarized rod-like conformations, with λ_{max}'s of 430 and 550 nm, respectively.[48]

The emergence of a weak vibronic fine structure at 590 nm appears in the rod-like state of the complex, which is distinctly different from that of pristine P3KHT aggregates in water (Figure 1a); the relative absorptivity at 590 nm is much weaker in the complex. It has been recognized that the backbone planarization of regioregular polythiophenes yields the vibronic fine structure with a lower electronic energy via single-molecule conformational extension.[49] The intensity of the lower energy absorption has been identified as indicative of planarization degree of the backbone.[43] We believe that the time-dependent red shift of λ_{max} from 430 to 550 nm is the result of conformational extensions of the individual complexes, whereas they remain little aggregated due to long alkyl side chains.

The intramolecular hypothesis is supported by in situ fluorescence data, as shown in Figure 3c. The emission maximum shows a 50 nm red shift with aging time, but no significant photoquenching is observed during the bathchromic shift. The Stokes shift, defined as the difference between emission and absorbance band maxima ($\Delta\lambda = \lambda_{em,max} - \lambda_{abs,max}$), is found to progressively decrease from the initial coil-like ($\Delta\lambda$ = 130 nm) to final rod-like conformation ($\Delta\lambda$ = 60 nm). Vibrational relaxations of the excited-state fluorophores in the supramolecular environment are therefore significantly reduced after the transition. The reduction in the Stokes shift energy, by nearly 0.5 eV, supports the significant extension of the backbone, which provides improved overlap of fluorophores and a lesser extent of nonradiative electronic transitions.[30,31]

These phenomena collectively demonstrate a coil-to-rod transition; polymer chains undergo a time-dependent conformational transition from a coil-like state, with twisting and bending between thiophene repeat units, to a rod-like state that has a smaller dihedral angle between thiophene rings, which yields an elongation of the effective conjugation length. In the rod-like conformation, surfactant side chains interact closely and resist free rotation of the thiophene units. The planarized backbone essentially minimizes the presence of charge-trapping kinks along the chain.[26] However, this rod-like conformation necessarily possesses a higher surface energy and is thermodynamically metastable.[12] Therefore, with much longer aging times, the polymer rods aggregate together to minimize the interfacial area, as evidenced by flaky precipitates of the complex after weeks (Figure 3a).

It should be noted that a time-dependent chromism of the complex was not observed in the concentrated stock hydrogels (Scheme 1c), even after months of storage. This is attributed to entanglements of the coil-like complex chains. Upon dilution, these chains are freed from entanglements. With aging time, the coil-like conformation will transform into the thermodynamically favored rod-like conformation. Since the complex possesses long alkyl side chains, $\pi-\pi$ stacking between the backbones is kinetically hindered and contributes to aggregation only with a sufficiently long aging period.

To further understand the mechanism of the coil-to-rod transition of the aqueous polymer complex, UV−vis absorption measurement is used to study the rate of time-dependent chromism of the solution with different concentrations (Figure 4). Interestingly, kinetics measurements display an inverse first-order rate law: the growth rate of the polymer rods is found to decline proportionally with concentration. The method of initial rates was used to determine the rate law and to calculate the rate constant,[50] as presented in Figure 4. Theoretically, the rate (R) is predicted to scale with concentration (C) as $R \propto C^n$, where the exponent determines the reaction order. The data points fall onto a line obeying the scaling relationship where $R \propto C^{-0.98\pm0.01}$ (Figure 4b). This inverse first-order relationship provides powerful evidence for the intrachain origin of the time-dependent chromism. Free of the high-viscosity environment in the gel, the more quickly the bulk of the chains can attain their thermodynamically favored extended conformation at room temperature. As solution concentration approaches that of the stock hydrogel, the initial rate approaches zero. This phenomenon is in contrast with that of P3HT in a marginal organic solvent. The latter consistently shows a direct proportionality to concentration.[51,52]

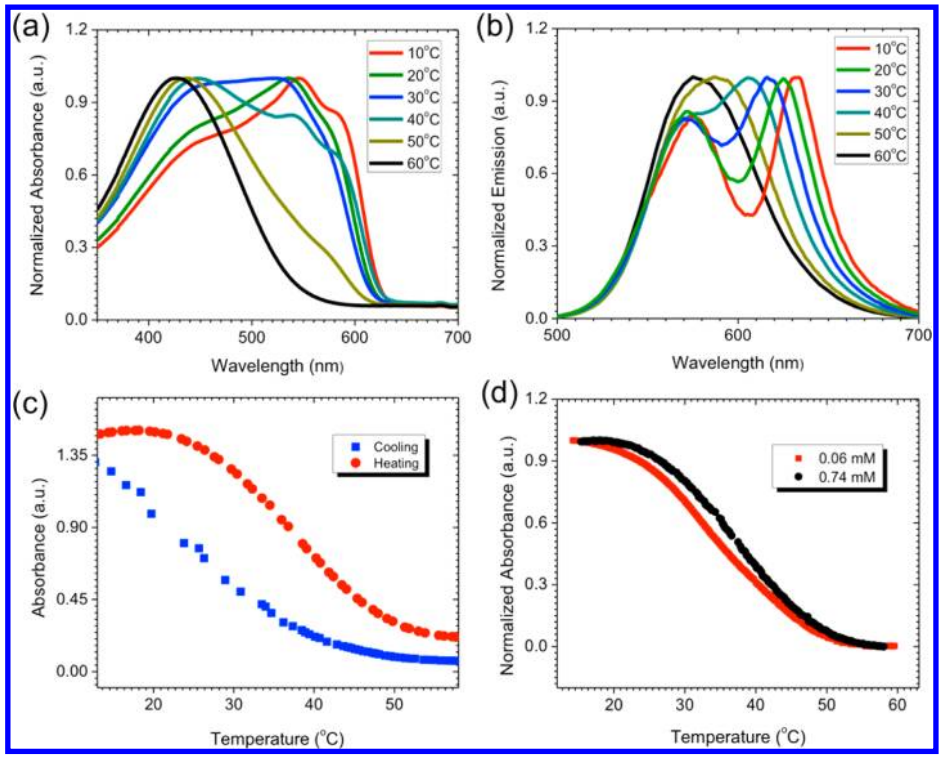

Figure 5. Thermochromism of the aqueous P3KHT−CTAB complex. (a) Absorption and (b) emission spectra (λ_{exc} = 430 nm). Measurements were performed during cooling for 30 min equilibration. The concentration is 4×10^{-5} M. (c) Temperature-dependent absorbance at λ = 590 nm. The scanning rate is 2 °C/min, and the concentration is 4×10^{-5} M. (d) Temperature-dependent absorbance at λ = 590 nm of the complex with different concentrations. The heating rate is 0.25 °C/min.

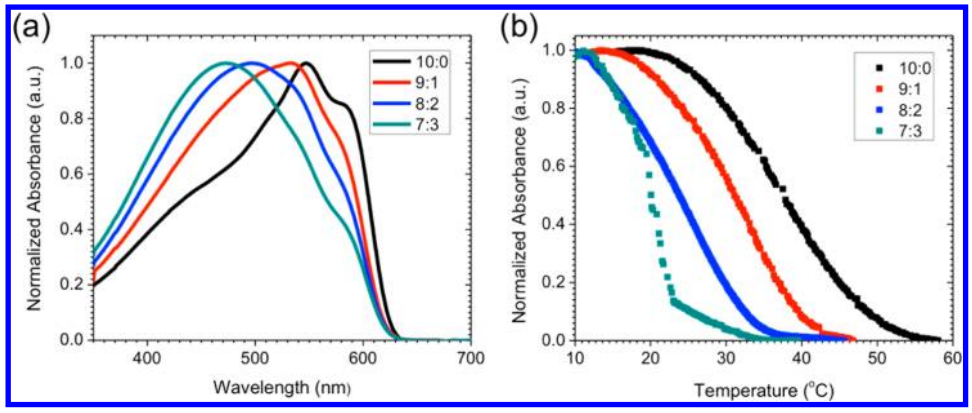

Figure 6. Effect of surfactant architecture on thermochromism. (a) Absorption spectra of the aqueous complexes with various side chain compositions at 30 °C after 30 min equilibration. (b) Temperature-dependent absorbance at λ = 590 nm of the aqueous complexes with various side chain compositions. The concentration is 2×10^{-5} M, and the heating rate is 0.25 °C/min. Ratios in the legend refer to the side chain proportion (CTAB/DHAB) in the charge-balanced complexes.

Figure 5 shows thermochromism of the aqueous complex in the dilute regime. At high temperature, the polymer chains adopt coil-like conformations to maximize the system's entropy, and thus, the absorption maximum shifts toward low wavelengths (Figure 5a). With decreasing temperature, below a critical value, the polymer chains transform from coil-like to rod-like conformations to minimize the total free energy. As a result, the absorption maximum shifts toward higher wavelengths (Figure 5a). Support along this line is provided by temperature-dependent fluorescence of the complex (Figure 5b). High temperatures induce lower wavelength emission, and lower temperatures result in a red shift of the emission. However, the control P3KHT in water shows no thermochromism in the temperature range of 10−60 °C.

It should be noted that the thermochromism of the complex is reversible, with the presence of rate-dependent hysteresis (Figure 5c). For this reason, the critical transition temperature was calculated via quasistatic approximation, that is, in dilute solutions at infinitesimally slow scan rates. The critical temperature for the P3KHT-CTAB complex was calculated as T_c = 37 ± 3 °C, corresponding to the magnitude of the thermochromic function's first derivative ($|dA_{590}/dT|^{max}$). The sample standard deviation of repeated measurements is provided as the uncertainty because a slight variability between batches was observed. To further understand the origin of

dx.doi.org/10.1021/jp307728r | J. Phys. Chem. B 2012, 116, 12887−12894

Scheme 2. A Schematic Diagram of Possible Structural Changes during Chromism of the Aqueous P3KHT−CTAB Complexes[a]

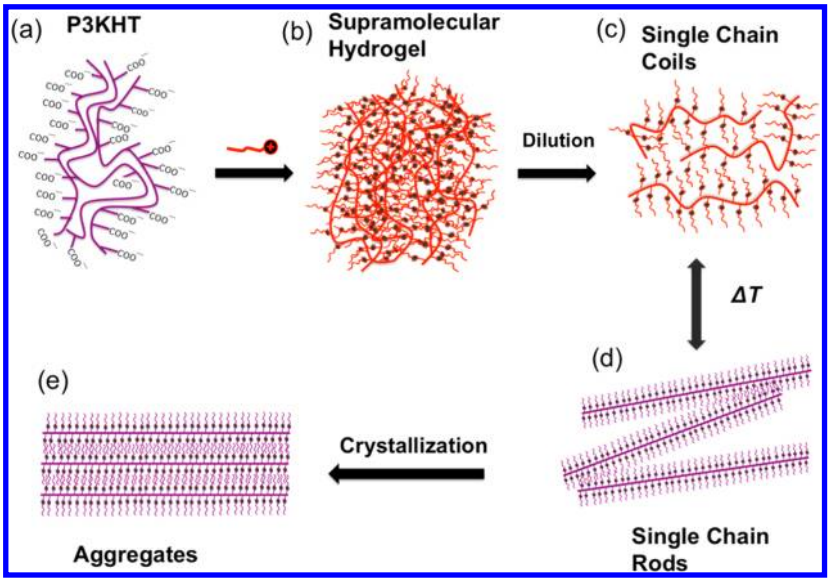

[a](a) Loose aggregates of pure P3KHT chains in water. (b) As-prepared hydrogels by complexation between P3KHT and CTAB. (c) Coil-like conformation of single polymer chains in the diluted solution. (d) Rod-like conformation of single polymer chains in the diluted solution. (e) Rod aggregates after long time standing.

transition mechanism, thermochromism of the aqueous complex with different concentrations has been investigated. Figure 5d shows thermochromism of 0.06 and 0.74 mM solutions during heating. Within experimental errors, the thermochromism is concentration-independent, indicating an intrachain mechanism of the coil−rod transition.[13] Therefore, the transition is intrinsic to each polymer molecule.

To investigate the effect of surfactant architecture on the critical transition temperature, T_c, a certain amount of the double-tail surfactant, dihexadecyl dimethyl ammonium bromide (DHAB), was added to the P3KHT−CTAB complexes. The molar ratio of total surfactants (CTAB and DHAB) and P3KHT carboxylate units is stoichiometric (charge-balanced) in these complexes. With an increasing amount of the DHAB, the room-temperature absorption maximum shifts toward lower wavelengths (Figure 6a). This suggests that more coil-like backbone structures are favored with a higher loading of DHAB. The T_c of each complex was found to decrease proportionally with an increase in the relative proportion of DHAB side chains, as shown in Figure 6b. These results indicate that the coil-like conformation is more favored in the complex with greater DHAB incorporation.

Mechanism. It is well recognized that the neutral P3HT chains adopt a coil-like conformation in good solvents. Upon addition of a poor solvent, P3HT chains undergo a structural transition from coil-like conformations to rod-like aggregates, accompanied by the formation of crystalline nanowires.[12,14] Polymer solubility due to polymer−solvent interactions plays a crucial role in this structural transition.[53] Studies on the kinetics and thermodynamics of solvent-induced P3HT nanowire crystallization have revealed a possible intra-/interchain two-step mechanism.[12,13,51,52] The first step is a coil-to-rod conformational transition of single polymer chains[13] in which backbones convert from a twisted coil-like state to a planar rod-like state, which yields an elongation of effective conjugation lengths. However, this rod-like species has a larger surface energy and is therefore metastable.[12] These rods will subsequently aggregate together via $\pi-\pi$ stacking to minimize their surface energy.[12] The first step, the conformational transition, is often too fast to be deconvoluted with respect to the optoelectronic properties of the system. The second step, aggregate formation, is the rate-determining step for polymer chromism.[51] As such, the kinetics and thermodynamics of aggregation/crystallization are used to describe polythiophene chromism.[12] For this reason, the dynamic behavior of crystalline nanowire growth rate against concentration obeys a first-order rate law.[51,52]

The chromism of the water-soluble P3HT derivative presented in this work is different from that of neutral P3HT in organic solvents: First, the time-dependent coil-to-rod transition occurs only in a newly diluted solution. Second, the dynamic process of time-dependent chromism follows an inverse first-order rate law. Scheme 2 is a proposed chromism mechanism based on these observations. The pure P3KHT chains are present as loose aggregates (Scheme 2a), analogous to other CPEs.[33] During complexation, the surfactants break up the P3KHT aggregates. The resultant coil-like complex chains entangle each other to form penetrated networks[54] (Scheme 2b). The chain entanglements serve as physical cross-linkers to stabilize as-prepared hydrogels. Therefore, the hydrogel is very stable at room temperature over months. Upon dilution, the coil-like chains are freed from entanglements[54] (Scheme 2c). Single polymer chains spontaneously transform from a coil-like to rod-like conformation (Scheme 2d). This process is an intrachain phenomenon[12,13] and can occur only below a critical transition temperature, T_c. This intrachain mechanism is strongly supported by the observed inverse first-order rate law (Figure 4b) and concentration-independent thermochromism (Figure 5d). Thus, the coil-to-rod transition of single chains in the polymer complex is a rate-determining step.

From a thermodynamic viewpoint, the rod-like state possesses less entropy and is enthalpically driven below T_c, where the system undergoes a spontaneous process to minimize free energy (ΔG). The coil-to-rod transition is therefore an exothermic process that ensues in the perturbed system below $T_c = \Delta H/\Delta S$ and is thermally reversible. With

dx.doi.org/10.1021/jp307728r | J. Phys. Chem. B 2012, 116, 12887−12894

increasing temperature, the increased entropy of the coil-like state thermodynamically "outweighs" the exothermic interactions present in the extended conformation. The entropic component of the system is believed to be driven by the reduction of the interfacial area of the complex (i.e., as a result of the hydrophobic effect), whereas the enthalpic component is mediated by the steric arrangement of the supramolecular side chains and resonance of coplanar thiophene units.[45]

The surfactant side chain architecture is crucial in determining T_c, as shown in Figure 6. The greater lipophilic nature of the complex, with more double-tail side chains, clearly contributes more to the entropy of the coil state because it results in a reduction of the critical transition temperature. The greater hydrophobicity was noted macroscopically, and the complex was not entirely soluble with high proportions of DHAB loading. The favorable reduction in interfacial area of the more hydrophobic complex (i.e., the favored coil-like state) with greater proportion of DHAB provides support for the initiation of aggregation via an intramolecular mechanism. Plain aggregation would be expected to be favorable at higher temperatures, with greater hydrophobicity of the complex, if such aggregation were not initiated by a prerequisite change in the complex's interfacial area.

Although the intrachain mechanism allows us to explain the optoelectronic phenomena successfully, an interchain mechanism is clearly indicated in the much later precipitation of the rod-like complex, in which the large surface area of the extended conformation makes it metastable.[12] However, we believe that the surface energy of the aqueous P3KHT complex in the rod-like state is not as rapid a driving force for aggregation when compared with that of neutral P3HT in an organic solvent because backbone interactions are kinetically hindered by the long alkyl side chains. Thus, the aggregation of polymer rods via $\pi-\pi$ stacking is much slower once the coil-to-rod transition of single chains has occurred (Scheme 2e).

CONCLUSIONS

In summary, we have in situ investigated the kinetics and thermodynamics of the surfactochromism of aqueous P3KHT–CTAB complexes. The diluted solution exhibits spontaneous time-dependent chromism at room temperature. Detailed analysis of the dynamic process reveals an inverse first-order rate law of the phase transition. Temperature-dependent chromism is completely reversible and is concentration-independent. An intrachain mechanism is proposed on the basis of the observed phenomena. Single polymer chains under perturbed conditions spontaneously transform from a twisted coil-like conformation into a planar rod-like conformation. Surfactant architecture is crucial for determining such critical transition temperatures. Our work addresses an important fundamental issue concerning surfactant-induced ordering of nanostructures for water-soluble conjugated polymers. Because of an emerging demand for ordered nanostructures of water-soluble conjugated polymers in high-efficiency flexible optoelectronic devices, our work represents a scientific foundation for green processing in the manufacture of such functional materials.

AUTHOR INFORMATION

Corresponding Author

*Phone: +1 805 756 2591. Fax: +1 805 756 5500. E-mail: szhang05@calpoly.edu.

Notes

The authors declare no competing financial interest.

ACKNOWLEDGMENTS

This work is supported by the Cal Poly Startup Fund and the State Faculty Support Grant.

REFERENCES

(1) Liu, Y.; Wang, H. F.; Dong, H. L.; Tan, J. H.; Hu, W. P.; Zhan, X. W. *Macromolecules* **2012**, *45* (3), 1296–1302.
(2) Brabec, C. J.; Gowrisanker, S.; Halls, J. J. M.; Laird, D.; Jia, S. J.; Williams, S. P. *Adv. Mater.* **2010**, *22* (34), 3839–3856.
(3) Chen, S.; Deng, L.; Xie, J.; Peng, L.; Xie, L.; Fan, Q.; Huang, W. *Adv. Mater.* **2010**, *22* (46), 5227–5239.
(4) Causin, V.; Marega, C.; Marigo, A.; Valentini, L.; Kenny, J. M. *Macromolecules* **2005**, *38* (2), 409–415.
(5) Lee, J. S.; Son, S. K.; Song, S.; Kim, H.; Lee, D. R.; Kim, K.; Ko, M. J.; Choi, D. H.; Kim, B.; Cho, J. H. *Chem. Mater.* **2012**, *24* (7), 1316–1323.
(6) Biniek, L.; Chochos, C. L.; Leclerc, N.; Boyron, O.; Fall, S.; Leveque, P.; Heiser, T. *J. Polym. Sci., Part A: Polym. Chem.* **2012**, *50* (9), 1861–1868.
(7) Tada, A.; Geng, Y. F.; Wei, Q. S.; Hashimoto, K.; Tajima, K. *Nat. Mater.* **2011**, *10* (6), 450–455.
(8) Minh Trung, D.; Hirsch, L.; Wantz, G. *Adv. Mater.* **2011**, *23* (31), 3597–3602.
(9) Ren, S.; Bernardi, M.; Lunt, R. R.; Bulovic, V.; Grossman, J. C.; Gradecak, S. *Nano Lett.* **2011**, *11* (12), 5316–5321.
(10) Lobez, J. M.; Andrew, T. L.; Bulovic, V.; Swager, T. M. *ACS Nano* **2012**, *6* (4), 3044–3056.
(11) Treat, N. D.; Brady, M. A.; Smith, G.; Toney, M. F.; Kramer, E. J.; Hawker, C. J.; Chabinyc, M. L. *Adv. Energy Mater.* **2011**, *1* (1), 82–89.
(12) Xu, W.; Li, L.; Tang, H.; Li, H.; Zhao, X.; Yang, X. *J. Phys. Chem. B* **2011**, *115* (20), 6412–6420.
(13) Rughooputh, S.; Hotta, S.; Heeger, A. J.; Wudl, F. *J. Polym. Sci., Part B: Polym. Phys.* **1987**, *25* (5), 1071–1078.
(14) Scharsich, C.; Lohwasser, R. H.; Sommer, M.; Asawapirom, U.; Scherf, U.; Thelakkat, M.; Neher, D.; Koehler, A. *J. Polym. Sci., Part B: Polym. Phys.* **2012**, *50* (6), 442–453.
(15) Rodd, C. M.; Agarwal, R. *Nano Lett.* **2011**, *11* (8), 3460–3467.
(16) Kim, J. S.; Lee, J. H.; Park, J. H.; Shim, C.; Sim, M.; Cho, K. *Adv. Funct. Mater.* **2011**, *21* (3), 480–486.
(17) Liu, F.; Gu, Y.; Jung, J. W.; Jo, W. H.; Russell, T. P. *J. Polym. Sci., Part B: Polym. Phys.* **2012**, *50* (15), 1018–1044.
(18) Ren, G.; Wu, P.-T.; Jenekhe, S. A. *ACS Nano* **2011**, *5* (1), 376–384.
(19) Yang, X. N.; Loos, J.; Veenstra, S. C.; Verhees, W. J. H.; Wienk, M. M.; Kroon, J. M.; Michels, M. A. J.; Janssen, R. A. J. *Nano Lett.* **2005**, *5* (4), 579–583.
(20) Hoven, C. V.; Garcia, A.; Bazan, G. C.; Thuc-Quyen, N. *Adv. Mater.* **2008**, *20* (20), 3793–3810.
(21) Huang, Y.; Fan, Q.; Wei, H. *Prog. Chem.* **2008**, *20* (4), 574–585.
(22) Wang, L.; Li, H.; Cao, D. *Curr. Org. Chem.* **2012**, *16* (12), 1468–1484.
(23) Lee, K.; Kim, H.-J.; Kim, J. *Adv. Funct. Mater.* **2012**, *22* (5), 1076–1086.
(24) Franco, I. E.; Lorchat, P.; Lamps, J. P.; Schmutz, M.; Schroeder, A.; Catala, J. M.; Combet, J.; Schosseler, F. *Langmuir* **2012**, *28* (10), 4815–4828.
(25) Duarte, A.; Pu, K.-Y.; Liu, B.; Bazan, G. C. *Chem. Mater.* **2011**, *23* (3), 501–515.
(26) Tennyson, A. G.; Christopher, J. W. K.; Bielawski., W. *Chem. Commun.* **2009**, *16*, 2124–2126.
(27) Zhang, S. J.; Pfefferle, L. D.; Osuji, C. O. *Macromolecules* **2010**, *43* (18), 7549–7555.
(28) Yang, S.-H.; Hsu, C.-S. *J. Polym. Sci., Part A: Polym. Chem.* **2009**, *47* (11), 2713–2733.

(29) Lavigne, J. J.; Broughton, D. L.; Wilson, J. N.; Erdogan, B.; Bunz, U. H. F. *Macromolecules* **2003**, *36* (20), 7409−7412.
(30) Chen, L. H.; Xu, S.; McBranch, D.; Whitten, D. *J. Am. Chem. Soc.* **2000**, *122* (38), 9302−9303.
(31) Knaapila, M.; Evans, R. C.; Garamus, V. M.; Almasy, L.; Szekely, N. K.; Gutacker, A.; Scherf, U.; Burrows, H. D. *Langmuir* **2010**, *26* (19), 15634−15643.
(32) Knaapila, M.; Evans, R. C.; Gutacker, A.; Garamus, V. M.; Szekely, N. K.; Scherf, U.; Burrows, H. D. *Soft Matter* **2011**, *7* (15), 6863−6872.
(33) Laurenti, M.; Rubio-Retama, J.; Garcia-Blanco, F.; Lopez-Cabarcos, E. *Langmuir* **2008**, *24* (23), 13321−13327.
(34) Al Attar, H. A.; Monkman, A. P. *J. Phys. Chem. B* **2007**, *111* (43), 12418−12426.
(35) Chu, B.; Xu, R. L. *Acc. Chem. Res.* **1991**, *24* (12), 384−389.
(36) Lanzi, M.; Paganin, L. *Eur. Polym. J.* **2008**, *44* (12), 3987−3996.
(37) Treger, J. S.; Ma, V. Y.; Gao, Y.; Wang, C.-C.; Wang, H.-L.; Johal, M. S. *J. Phys. Chem. B* **2008**, *112* (3), 760−763.
(38) Li, W.; Worfolk, B. J.; Li, P.; Hauger, T. C.; Harris, K. D.; Buriak, J. M. *J. Mater. Chem.* **2012**, *22* (22), 11354−11363.
(39) Worfolk, B. J.; Rider, D. A.; Elias, A. L.; Thomas, M.; Harris, K. D.; Buriak, J. M. *Adv. Funct. Mater.* **2011**, *21* (10), 1816−1826.
(40) McClure, S. A.; Worfolk, B. J.; Rider, D. A.; Tucker, R. T.; Fordyce, J. A. M.; Fleischauer, M. D.; Harris, K. D.; Brett, M. J.; Buriak, J. M. *ACS Appl. Mater. Interfaces* **2010**, *2* (1), 219−229.
(41) Zhang, S.; Pelligra, C. I.; Keskar, G.; Jiang, J.; Majewski, P. W.; Taylor, A. D.; Ismail-Beigi, S.; Pfefferle, L. D.; Osuji, C. O. *Adv. Mater.* **2012**, *24* (1), 82−87.
(42) Conio, G.; Bianchi, E.; Ciferri, A.; Krigbaum, W. R. *Macromolecules* **1984**, *17* (4), 856−861.
(43) Wu, M.-C.; Lin, Y.-Y.; Chen, S.; Liao, H.-C.; Wu, Y.-J.; Chen, C.-W.; Chen, Y.-F.; Su, W.-F. *Chem. Phys. Lett.* **2009**, *468* (1−3), 64−68.
(44) Zhao, X. Y.; Schanze, K. S. *Langmuir* **2006**, *22* (10), 4856−4862.
(45) Tapia, M. J.; Burrows, H. D.; Knaapila, M.; Monkman, A. P.; Arroyo, A.; Pradhan, S.; Scherf, U.; Pinazo, A.; Perez, L.; Moran, C. *Langmuir* **2006**, *22* (24), 10170−10174.
(46) Viinikanoja, A.; Areva, S.; Kocharova, N.; Aaritalo, T.; Vuorinen, M.; Savunen, A.; Kankare, J.; Lukkari, J. *Langmuir* **2006**, *22* (14), 6078−6086.
(47) Crossland, E. J. W.; Tremel, K.; Fischer, F.; Rahimi, K.; Reiter, G.; Steiner, U.; Ludwigs, S. *Adv. Mater.* **2012**, *24* (6), 839−844.
(48) Roux, C.; Leclerc, M. *Macromolecules* **1992**, *25* (8), 2141−2144.
(49) Adachi, T.; Lakhwani, G.; Traub, M. C.; Ono, R. J.; Bielawski, C. W.; Barbara, P. F.; Vanden Bout, D. A. *J. Phys. Chem. B* **2012**, *116* (32), 9866−72.
(50) Hall, K. J.; Quickenden, T. I.; Watts, D. W. *J. Chem. Educ.* **1976**, *53* (8), 493−494.
(51) Malik, S.; Jana, T.; Nandi, A. K. *Macromolecules* **2001**, *34* (2), 275−282.
(52) Liu, J.; Zou, J.; Zhai, L. *Macromol. Rapid Commun.* **2009**, *30* (16), 1387−1391.
(53) Park, Y. D.; Lee, S. G.; Lee, H. S.; Kwak, D.; Lee, D. H.; Cho, K. *J. Mater. Chem.* **2011**, *21* (7), 2338−2343.
(54) Litmanovich, E. A.; Zakharchenko, S. O.; Stoichev, G. V. *J. Phys. Chem. B* **2007**, *111* (29), 8567−8571.